

Received 1 March 2021; revised 11 May 2021; accepted 14 June 2021. Date of publication 17 June 2021; date of current version 25 June 2021.
The review of this article was arranged by Editor M. K. Radhakrishnan

Digital Object Identifier 10.1109/JEDS.2021.3090091

Gate Failure Behavior and Mechanism of AlGaN/GaN HEMTs Under Transmission Line Pulsed Stress

Y. REN, Y. Q. CHEN¹ (Member, IEEE), C. LIU¹, X. B. XU¹, R. GAO¹, D. Y. LEI¹ (Member, IEEE),
P. LAI, Y. HUANG (Member, IEEE), AND J. HE

No.5 Electronics Research Institute, Ministry of Industry and Information Technology Guangzhou, Guangdong 510610, China

CORRESPONDING AUTHORS: Y. Q. Chen AND C. Liu (e-mail: chen@hotmail.com; xd_liuchang@163.com)

This work was supported by the Key Realm R&D Program of Guangdong Province under Grant 2020B010171002, Grant 2020B010173001, Grant 2018B010142001, and Grant 2019B010143002.

ABSTRACT The failure behavior and the corresponding physical mechanism of the AlGaN/GaN high electron mobility transistors (HEMTs) under transmission line pulse (TLP) stress were investigated in this paper. The result shows that the output and transfer characteristics of the AlGaN/GaN HEMTs after 90 cycles begin to degrade by comparing with the fresh ones under 40 V TLP voltage, and the gate leakage current of the devices slightly increases. When the TLP voltage of 52 V was applied, a catastrophic failure occurs for the AlGaN/GaN HEMTs. Furthermore, the failure of the AlGaN/GaN HEMTs was located, and the micro-morphology of the abnormal spot was observed. The result shows that the gate metal was damaged due to the large TLP stress. The failure mechanism may be mainly attributed to the Joule heat that causes the high lattice temperature of 1160 K as well as the electric field, and it is higher than the melting point of Au (1064 K) in the gate metal (Au/Ti/Mo). The results may be useful in the design and application of electrostatic discharge (ESD) for AlGaN/GaN HEMTs.

INDEX TERMS GaN HEMT, failure, transmission line pulse.

I. INTRODUCTION

AlGaN/GaN high electron mobility transistors (HEMTs) are promising devices for application in the high-temperature, high-frequency, and high-power fields. It is well-known that AlGaN/GaN HEMTs own wide bandgap, high breakdown electric field, and high two-dimensional electron gas (2DEG) concentration. Therefore, AlGaN/GaN HEMTs have been recognized as excellent devices. [1]–[4]. As we already know, the effect of electrostatic discharge (ESD) on device stability and reliability is very important, especially the AlGaN/GaN HEMTs are applied to high power electronics [5]. Despite the high breakdown field of GaN (3.3 MV/cm), transistors based on GaN are still threatened due to ESD [6], [7]. Devices are placed in the high voltages or currents during ESD events leading to their failure eventually. The sensitivity of III-V compounds to the ESD events [6], [8] contributes to defining ESD protection as a serious reliability problem before the emerging GaN technology can be widely used in the consumer market [9]–[11]. Despite

the importance of ESD reliability issues for GaN-based HEMT devices, there are a few results reported in the literature. Kuzmík *et al.* [12], [13] had investigated the effect of drain-source current (I_{DS}) on the ESD of AlGaN/GaN HEMTs. When the I_{DS} was low, the electrical characteristics of the devices would not change in the snapback work regime. In the case of the floating gate, the I_{DS} of tested devices can reach 1.6 A, and Schottky contact of the device was not degenerate. However, when I_{DS} was exceeding 1.6 A, the electrical characteristic of the devices begins to change. A catastrophic failure was observed with the filament formation. Tazzoli *et al.* [14] had tested the robustness of the different configurations of AlGaN/GaN HEMTs in ESD events. The two failure mechanisms of devices have identified for the degradation of the gate-source diode and the formation of filaments, and they had investigated the failure current scales with the width of devices. Rossetto *et al.* [6] had investigated the robustness of the ESD and failure mechanisms of AlGaN/GaN HEMTs.

Transmission line pulse (TLP) was applied to the drain under gate OFF-state conditions that failure of the devices had been appeared due to a field-dependent mechanism. On the contrary, when the pulse was used to the drain under gate ON-state conditions that a power-dependent mechanism had occurred. Finally, they have proved that the length of the field plate can affect the ESD characteristic of the devices and vertical (drain substrate) breakdown of the devices would not be affected for the ESD stability.

In the paper, the electrical properties of AlGaN/GaN HEMTs before and after the ESD stress by transmission line pulse were investigated. Considering that our research group has carried out some studies on the negative TLP stress of GaN HEMT gate in previous work [15], [16], therefore, the positive TLP stress was studied in this time. In addition to degradation, we also focus on the tolerance limit of the device to the positive TLP stress and its failure mechanism. The failure region has been verified through emission microscope (EMMI). Moreover, the failure phenomena and the failure mechanism of AlGaN/GaN HEMTs were analyzed using scanning electron micrograph (SEM) and simulation method. The results may provide useful guidelines in the application of ESD protection of AlGaN/GaN HEMTs.

II. EXPERIMENTS

The device structure of AlGaN/GaN HEMTs was shown in Fig. 1. The simple schematic diagram of the cross section of the AlGaN/GaN HEMTs was shown in Fig. 1(a), and the structure consists of a 40 nm AlN nucleation layer, a 3 μm thick GaN buffer layer, a 20 nm $\text{Al}_{0.2}\text{Ga}_{0.8}\text{N}$ barrier layer, a 10 nm GaN cap layer, and a GaN transition layer grown on the SiC substrate. The devices have a gate width of 1.25 mm, a gate length of 0.1 μm , a gate-drain spacing of 5 μm , and a gate-source spacing of 2 μm . The surface of the devices was passivated by a SiN_x layer of 150 nm. The schematic diagram of the TLP test is shown in Fig. 1(b), and the whole test system mainly consists of an oscilloscope, transmission line, devices under test (DUT), high voltage power, and matching resistance. The electrical parameters of DUTs were tested by a semiconductor device analyzer (Agilent B1500A). The pulse was applied to the DUTs by using TLP (TDR-TLP). The emission microscope was performed using Andor IXON 3 model 897 under a semi-ON state for the AlGaN/GaN HEMTs. Finally, the micro-morphology of the failure device was analyzed by HITACHI S-4300 SEM.

III. RESULTS AND DISCUSSION

A. ELECTRICAL CHARACTERISTICS OF ALGAN/GAN HEMTs UNDER TLP STRESS

Fig. 2 shows a typical TLP stress application of AlGaN/GaN HEMTs. From Fig. 2(a), the parasitic capacitors C_{GS} (between gate and source) and C_{GD} (between gate and drain) were illustrated, along with the intrinsic gate-drain and gate-source Schottky diodes. The positive voltage pulses of 100 ns width were applied to the gate of devices, with source grounded, and drain floating. We chose G-S junction to apply

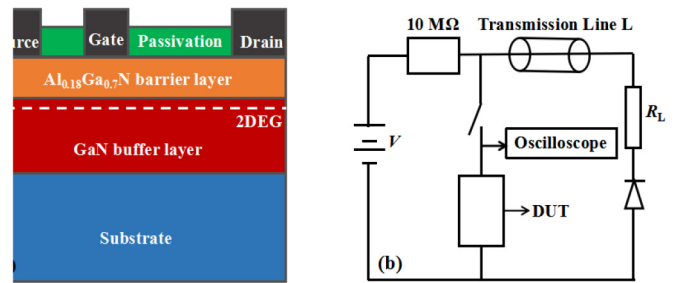


FIGURE 1. (a) the schematic diagram of cross section of device and (b) TLP test system.

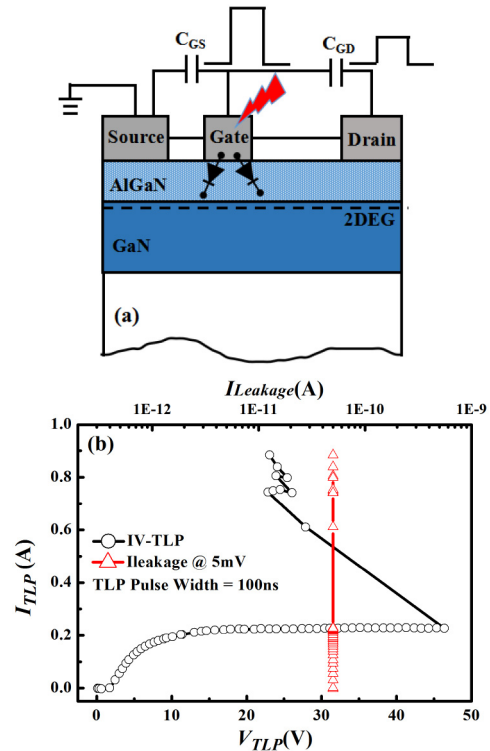


FIGURE 2. The typical TLP stress application of AlGaN/GaN HEMTs: (a) mechanism schematic of TLP stress acting on devices and (b) IV-TLP curve of devices stressed between gate and source, with drain floating.

TLP stress because compared with larger G-D length, G-S length is smaller and G-S junction has weaker ability to resist high voltage. Therefore, the degradation phenomena of G-S junction under TLP stress is the most critical and worthy of attention. As shown in Fig. 2(b), the average current and voltage waveform with pulse width was plotted. When the TLP voltage was less than 46 V, the TLP current was in a stable state. However, when the TLP voltage and current increased to 46 V and 0.2 A, respectively, there takes on a snapback point. The TLP voltage suddenly decreased to 29 V and the TLP current increased to 0.6 A. A catastrophic failure occurs just at the first snapback point. At each step interval of TLP stress, the test system automatically switches to measuring voltage to obtain gate-to-source leakage current (I_{GS}). The leakage current was measured at a low bias voltage state

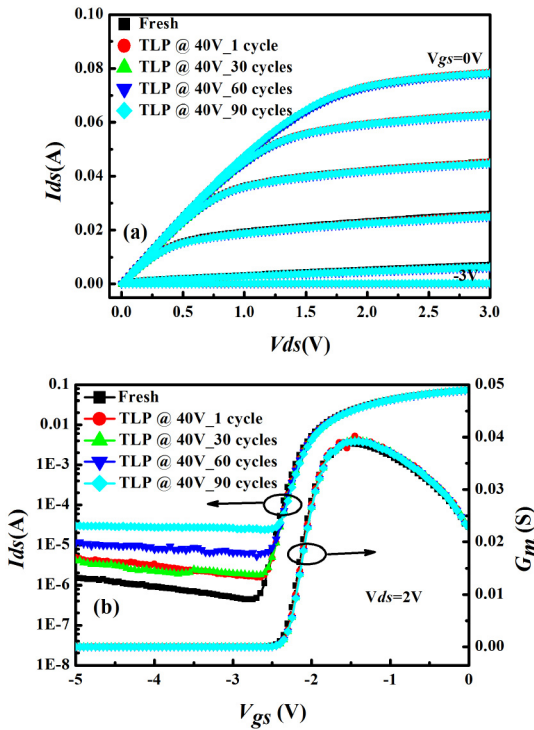


FIGURE 3. The typical DC characteristics of AlGaN/GaN HEMTs before and after TLP stress: (a) output characteristics of the devices with gate-to-source voltage ranging from -3.0 to 0 V at 0.5 V step, and (b) transfer characteristics and transconductance of the devices with drain-to-source voltage of 2 V.

(5 mV) to be able to assess the degradation and catastrophic failure [7], [14], [17]–[20]. Even if the devices were failure, the I_{GS} current was also unchanged in the work [14], [17].

To investigate the effect of TLP stress on the electrical properties of AlGaN/GaN HEMTs, the output characteristics, transfer characteristics and transconductance were measured before and after the TLP stress, as shown in Fig. 3. The DC characterization is done immediately after TLP pulse. The output characteristics of the fresh AlGaN/GaN HEMTs shows no obvious variation from the device after TLP stress of 40 V, and the number of TLP stress is ranging from 1 to 90 cycles with a step of 30 cycles. In addition, the gate-to-source voltage (V_{GS}) was ranging from -3 to 0 V with a step of 0.5 V as shown in Fig. 3(a). Similarly, the transconductance and threshold voltage of AlGaN/GaN HEMTs were obtained before and after the TLP stress as shown in Fig. 3(b). On the contrary, the I_{DS} after TLP stress become larger when V_{GS} is lower than -2.7 V. It indicates that there is degradation on the gate-source and gate-drain Schottky diodes [14], [21]–[23]. This phenomenon will increase the quiescent dissipation obviously. For the system, the increased quiescent dissipation of devices may lead to unnecessary waste of energy.

The gate-leakage currents of the fresh AlGaN/GaN HEMTs were tested before and after TLP stress as shown in Fig. 4. From Fig. 4(a), a slight variation could be observed on

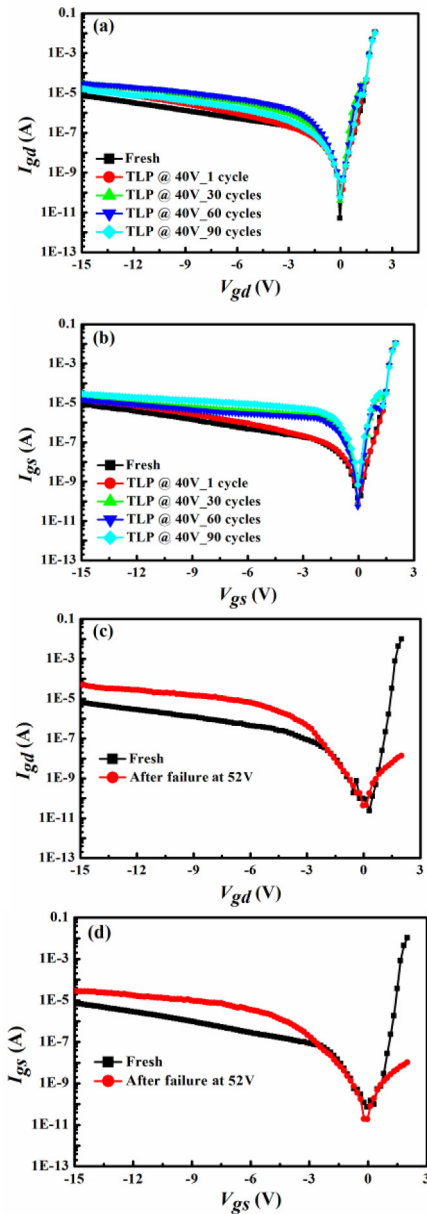


FIGURE 4. Schottky characteristics after TLP stress: (a) I_{gd} - V_{gd} and (b) I_{gs} - V_{gs} for the fresh devices, (c) I_{gd} - V_{gd} and (d) I_{gs} - V_{gs} for the gate failure of the device.

the gate-to-drain current (I_{GD}) of the AlGaN/GaN HEMTs before and after TLP voltage of 40 V. After the TLP stress, the gate-leakage current has slightly increased. As shown in Fig. 4(b), an obvious change could be observed on the gate-to-source current (I_{GS}) of fresh AlGaN/GaN HEMTs before and after TLP voltage of 40 V, the gate-leakage current increased obviously with the increase of TLP stress cycles. From Fig. 4(c), there is also an obvious variation on the I_{GD} of AlGaN/GaN HEMTs before and after the failure at 52 V. Compared with the fresh AlGaN/GaN HEMTs, the gate-to-drain current of the devices after failure varies greatly with V_{GD} at -15 V to -3 V, and has hardly change

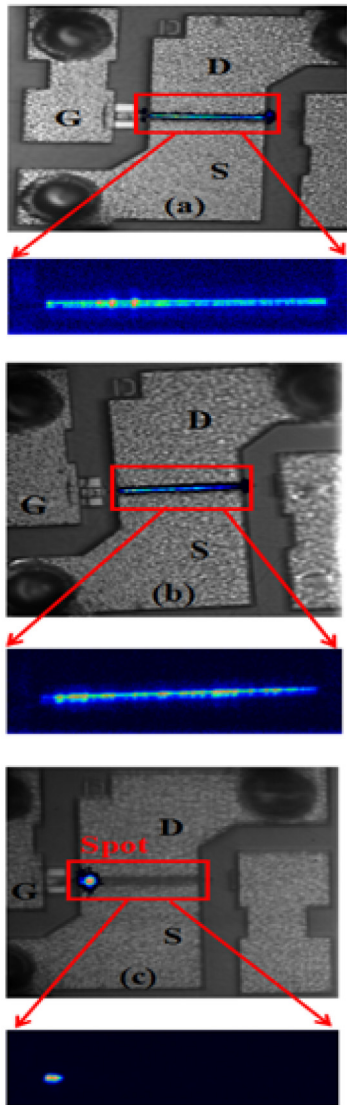


FIGURE 5. The EL intensity characterization of AlGaN/GaN HEMTs: (a) fresh device, (b) the device after TLP stress of 40 V and (c) the device TLP stress of 52 V.

with V_{GD} at -3 V to 0 V. As shown in Fig. 4(d), the obvious variation could be observed on the I_{GS} of AlGaN/GaN HEMTs before and after the failure at 52V, the variation of the I_{GS} is similar to the I_{GD} in Fig. 4(c). The results indicate that the gate-leakage current would be seriously affected by TLP stress.

B. EMMI ANALYSIS OF ALGAN/GAN HEMTS

To investigate the failure position of the AlGaN/GaN HEMTs after the TLP stress, the electroluminescence (EL) was carried out before and after TLP stress with the drain-to-source voltage of 5 V and V_{GS} of -2 V. The experimental results are shown in Fig. 5. The EL intensity of the fresh AlGaN/GaN (V_{DS}) HEMTs were obtained as shown in Fig. 5(a), and it is obvious that the EL intensity of the fresh devices is

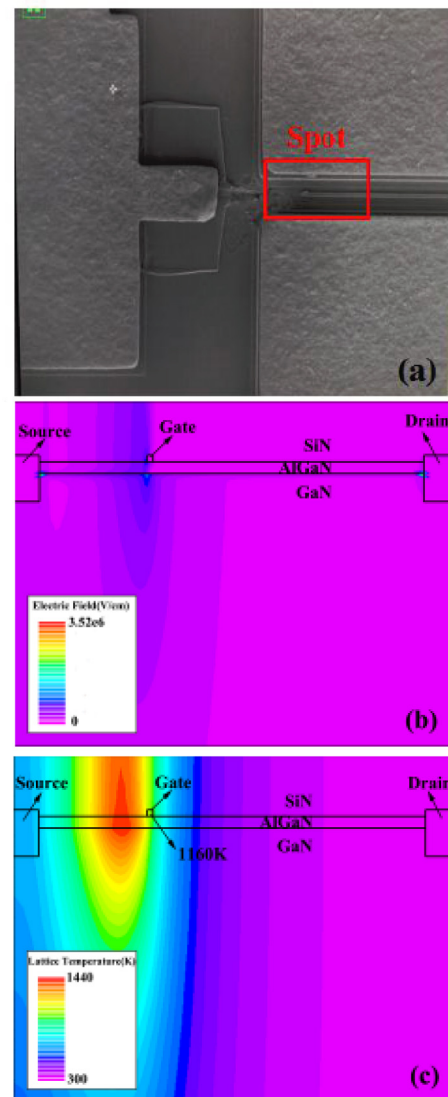


FIGURE 6. (a) SEM image, (b) electron field and (c) lattice temperature of AlGaN/GaN HEMTs after TLP stress of 52 V.

almost uniform, indicating that the devices own a good electrical characteristic. As shown in Fig. 5(b), after applying 40 V TLP voltage to the AlGaN/GaN HEMTs for 90 cycles, the EL intensity of the devices is almost uniform as well. The EMMI results are consistent with the DC characteristics shown in Fig. 3 in which no variation of the drain current is observed in the same bias point. As shown in Fig. 5(c), the EL intensity of the devices was uneven compared with that in Figs. 5(a) and (b). A light spot was obviously observed after the TLP stress of 52 V, and the catastrophic failure of the AlGaN/GaN HEMTs may be related to this spot.

C. DAMAGE MICRO-MORPHOLOGY AND FAILURE MECHANISM ANALYSIS OF ALGAN/GAN HEMTS AFTER TLP STRESS

In order to further understand the failure mechanism of AlGaN/GaN HEMTs after TLP stress, SEM experiments were performed on the areas where the abnormal light spot

[see Fig. 5(c)] of the sample appear in the EMMI analysis, as shown in Fig. 6(a). When the TLP stress of 52 V was applied to the gate of the AlGaN/GaN HEMT, the device failed catastrophically. It could be seen that the gate metal at the light spot in the red area was seriously damaged. In other words, the damage as well as the failure will occur due to the high TLP stress that is larger than the critical breakdown voltage. The electro-thermal simulation was carried out, and the results are shown in Figs. 6(b) and (c). The TLP stress is simulated by applying a transient voltage pulse from 0V to 52V to the gate of the device. The voltage pulse width is set to 100ns, which is consistent with the experiment. The electric field and lattice temperature distribution in the device was simulated by heat generation model and lattice heat transfer model at the end of the transient pulse. From Fig. 6(b), the simulation result shows that the maximum of electric field is about 3.52 MV/m at the drain and source terminal, which is lower than breakdown electric field of the AlGaN and larger than that of GaN materials (3.3 MV/m). From Fig. 6(c), the simulation result shows that the maximum of lattice temperature near the gate is up to 1160 K, which is lower than the melting point of Ti, Mo, AlGaN and GaN materials. However, it is higher than that of the Au, which is 1064 K. As the gate metal consists of Au, Ti and Mo, the failure mechanism may be attributed to the Joule heat as well as the electric field due to the TLP stress. In a word, the gate degradation of the device could be observed due to the several cycles of TLP voltage stress that is lower than the snapback point. Furthermore, the gate failure of the device will occur due to the Joule heat and electric field because of the TLP stress (52 V) that is higher than the snapback point voltage.

IV. CONCLUSION

In this work, we have investigated the failure mode and its mechanism of AlGaN/GaN HEMTs under gate-to-source TLP stress. When the positive voltage pulses of 100 ns pulse width were applied to the gate of the devices with source grounded and drain floating, we have observed that the output and transfer characteristics of AlGaN/GaN HEMTs degrade less after TLP voltage of 40 V. The gate-leakage current slightly increases with the TLP stress cycles. Instead, a catastrophic failure occurs for the AlGaN/GaN HEMTs under the TLP stress of 52 V. Through further analysis based on EMMI and SEM, it was found that a light spot was observed near the gate and the structural damage was observed. The gate metal was serious damaged due to the high TLP stress, and the failure mechanism may be mainly attributed to the Joule heat as well as the electric field. The results may provide useful guidelines in the ESD application of AlGaN/GaN HEMTs.

REFERENCES

[1] O. Ambacher *et al.*, "Two dimensional electron gases induced by spontaneous and piezoelectric polarization in undoped and doped AlGaIn/GaN heterostructures," *J. Appl. Phys.*, vol. 87, no. 1, pp. 334–344, Jan. 2000, doi: [10.1063/1.371866](https://doi.org/10.1063/1.371866).

[2] J. T. Asubar *et al.*, "Current collapse reduction in AlGaIn/GaN HEMTs by high-pressure water vapor annealing," *IEEE Trans. Electron Devices*, vol. 62, no. 8, pp. 2423–2428, Aug. 2015, doi: [10.1109/TEDE.2015.2440442](https://doi.org/10.1109/TEDE.2015.2440442).

[3] M. Ishida, T. Ueda, T. Tanaka, and D. Ueda, "GaN on Si technologies for power switching devices," *IEEE Trans. Electron Devices*, vol. 60, no. 10, pp. 3053–3059, Oct. 2013, doi: [10.1109/TEDE.2013.2268577](https://doi.org/10.1109/TEDE.2013.2268577).

[4] O. Hilt, P. Kotara, F. Brunner, A. Knauer, R. Zhytnytska, and J. Wurfl, "Improved vertical isolation for normally-off high voltage GaN-HFETs on n-SiC substrates," *IEEE Trans. Electron Devices*, vol. 60, no. 10, pp. 3084–3090, Oct. 2013, doi: [10.1109/TEDE.2013.2259492](https://doi.org/10.1109/TEDE.2013.2259492).

[5] A. Vescan *et al.*, "AlGaIn/GaN HFETs on 100 mm silicon substrates for commercial wireless applications," *Physica Status Solidi (c)*, vol. 0, no. 1, pp. 52–56, Jan. 2003, doi: [10.1002/pssc.200390106](https://doi.org/10.1002/pssc.200390106).

[6] I. Rossetto *et al.*, "Demonstration of field- and power-dependent ESD failure in AlGaIn/GaN RF HEMTs," *IEEE Trans. Electron Devices*, vol. 62, no. 9, pp. 2830–2836, Sep. 2015, doi: [10.1109/TEDE.2015.2463713](https://doi.org/10.1109/TEDE.2015.2463713).

[7] A. Amerasekera and C. Duvvury, "ESD in silicon integrated circuits," *Electron. Commun. Eng. J.*, vol. 9, no. 5, p. 208, Nov. 2002, doi: [10.1002/0470846054](https://doi.org/10.1002/0470846054).

[8] G. Meneghesso, A. Chini, A. Maschietto, E. Zanoni, P. Malberti, and M. Ciappa, "Electrostatic discharge and electrical overstress on GaN/InGaIn light emitting diodes," in *Proc. IEEE Elect. Overstress/Electrostatic Discharge Symp.*, Portland, OR, USA, Oct. 2001, pp. 247–252.

[9] K. Bock, "ESD issues in compound semiconductor high-frequency devices and circuits," *Microelectron. Rel.*, vol. 38, no. 11, pp. 1781–1793, Nov. 1998, doi: [10.1016/S0026-2714\(98\)00181-4](https://doi.org/10.1016/S0026-2714(98)00181-4).

[10] G. Meneghesso, A. Chini, M. Maretti, and E. Zanoni, "Pulsed measurements and circuit modeling of weak and strong avalanche effects in GaAs MESFETs and HEMTs," *IEEE Trans. Electron Devices*, vol. 50, no. 2, pp. 324–332, Feb. 2003, doi: [10.1109/TEDE.2003.809037](https://doi.org/10.1109/TEDE.2003.809037).

[11] A. Tazzoli, I. Rossetto, E. Zanoni, D. Yufeng, T. Tomasi, and G. Meneghesso, "ESD sensitivity of a GaAs MMIC microwave power amplifier," *Microelectron. Rel.*, vol. 51, nos. 9–11, pp. 1602–1607, Sep./Nov. 2011, doi: [10.1016/j.microrel.2011.06.051](https://doi.org/10.1016/j.microrel.2011.06.051).

[12] J. Kuzmík, D. Pogany, E. Gornik, P. Javorka, and P. Kordoš, "Electrical overstress in AlGaIn/GaN HEMTs: Study of degradation processes," *Solid-State Electron.*, vol. 48, no. 2, pp. 271–276, Feb. 2004, doi: [10.1016/S0038-1101\(03\)00295-8](https://doi.org/10.1016/S0038-1101(03)00295-8).

[13] J. Kuzmík, D. Pogany, and E. Gornik, "Electrostatic discharge effects in AlGaIn/GaN high-electron-mobility transistors," *Appl. Phys. Lett.*, vol. 83, no. 22, pp. 4655–4657, Dec. 2003, doi: [10.1063/1.1633018](https://doi.org/10.1063/1.1633018).

[14] A. Tazzoli, F. Danesin, E. Zanoni, and G. Meneghesso, "ESD robustness of AlGaIn/GaN HEMT devices," in *Proc. 29th Elect. Overstress/Electrostatic Discharge Symp. (EOS/ESD)*, Anaheim, CA, USA, Oct. 2007, pp. 1–9, doi: [10.1109/EOESD.2007.4401762](https://doi.org/10.1109/EOESD.2007.4401762).

[15] X. B. Xu *et al.*, "Analysis of trap and recovery characteristics based on low-frequency noise for E-mode GaN HEMTs under electrostatic discharge stress," *IEEE J. Electron Devices Soc.*, vol. 9, pp. 89–95, 2020, doi: [10.1109/jeds.2020.3040445](https://doi.org/10.1109/jeds.2020.3040445).

[16] Y. Q. Chen *et al.*, "Degradation behavior and mechanisms of E-mode GaN HEMTs with p-GaN gate under reverse electrostatic discharge stress," *IEEE Trans. Electron Devices*, vol. 67, no. 2, pp. 566–570, Feb. 2020, doi: [10.1109/teD.2019.2959299](https://doi.org/10.1109/teD.2019.2959299).

[17] Z. Wang, J. J. Liou, K.-L. Cho, and H.-C. Chiu, "Development of an electrostatic discharge protection solution in GaN technology," *IEEE Electron Device Lett.*, vol. 34, no. 12, pp. 1491–1493, Dec. 2013, doi: [10.1109/LED.2013.2283865](https://doi.org/10.1109/LED.2013.2283865).

[18] C. Zeng *et al.*, "Investigation of abrupt degradation of drain current caused by under-gate crack in AlGaIn/GaN high electron mobility transistors during high temperature operation stress," *J. Appl. Phys.*, vol. 118, Sep. 2015, Art. no. 124511, doi: [10.1063/1.4931891](https://doi.org/10.1063/1.4931891).

[19] L. B. Li, J. Joh, J. A. del Alamo, and C. V. Thompson, "Spatial distribution of structural degradation under high-power stress in AlGaIn/GaN high electron mobility transistors," *Appl. Phys. Lett.*, vol. 100, no. 17, p. 1022, Apr. 2013, doi: [10.1063/1.4707163](https://doi.org/10.1063/1.4707163).

[20] Y. Q. Chen *et al.*, "Degradation mechanism of AlGaIn/GaN HEMTs during high temperature operation stress," *Semicond. Sci. Technol.*, vol. 33, Nov. 2017, Art. no. 015019, doi: [10.1088/1361-6641/aa9d71](https://doi.org/10.1088/1361-6641/aa9d71).

[21] H. Jung *et al.*, "Reliability behavior of GaN HEMTs related to Au diffusion at the Schottky interface," *Physica Status Solidi*, vol. 6, no. S2, pp. S976–S979, Jun. 2010, doi: [10.1002/pssc.200880819](https://doi.org/10.1002/pssc.200880819).

[22] D. Marcon *et al.*, "Reliability analysis of permanent degradations on AlGaIn/GaN HEMTs," *IEEE Trans. Electron Devices*, vol. 60, no. 10, pp. 3132–3141, Oct. 2013, doi: [10.1109/TEDE.2013.2273216](https://doi.org/10.1109/TEDE.2013.2273216).

[23] Y. Koyama, T. Hashizume, and H. Hasegawa, "Formation processes and properties of Schottky and ohmic contacts on n-type GaN for field effect transistor applications," *Solid-State Electron.*, vol. 43, no. 8, pp. 1483–1488, Aug. 1999, doi: [10.1016/S0038-1101\(99\)00093-3](https://doi.org/10.1016/S0038-1101(99)00093-3).